A Photoredox-Catalyzed Approach for Formal Hydride Abstraction to Enable C_{sp^3}–H Functionalization with Nucleophilic Partners

Yufei Zhang[†], Nicholas A. Fitzpatrick[†], Mrinmoy Das[†], Ishani P. Bedre[†], Hatice G. Yayla[‡], Manjinder S. Lall[‡], Patricia Z. Musacchio[†]*

[†]Worcester Polytechnic Institute, 100 Institute Road, Worcester, MA 01609, USA. [‡]Pfizer Worldwide Research and Development, 445 Eastern Point Road, Groton, Connecticut 06340, USA.

While a great number of C_{sp^3}–H functionalization methods have been developed in recent years, new mechanistic paradigms to deconstruct these ubiquitous bonds have been comparatively rare. Of late, enabling C–H functionalization methods have relied on the intermediacy of a carbon radical intermediate to forge difficult C–C and C–X bonds. Strategies invoking a carbocation intermediate in the bond-forming step are less developed in the context of derivatizing C_{sp^3}–H bonds, likely due to the unfavorable thermodynamics of a direct hydride abstraction. Herein, we report our successful efforts in establishing a catalytic C_{sp^3}–H functionalization manifold for accessing reactive carbocation intermediates from a range of C_{sp^3}–H bonds. The novel catalytic design relies on a strategy driven by visible-light photoredox catalysis that combines two mechanistic steps in one catalytic cycle: hydrogen-atom transfer (HAT) and radical-polar crossover (RPC), formally accomplishing a net hydride abstraction. We herein initially demonstrated this new HAT-RPC platform in the context of C_{sp^3}–H fluorination by employing nucleophilic fluoride, a classically difficult nucleophile to engage. Difluorination of methylene groups is also demonstrated, and represents the first C–H difluorination with nucleophilic fluoride. Importantly, the carbocation intermediacy of the mechanistic design allows for the compatibility of the platform with several other classes of abundant nucleophile partners including halides, alcohols, water, amines, carboxylates, and arenes, an unachievable feat for open-shell intermediates without the use of a metal catalyst.

Introduction

Methods that can derivatize C_{sp^3}–H bonds to different functional groups have great potential to increase synthetic efficiency in the construction of complex small molecules or new therapeutic targets.[1]

The abundance of C_{sp}^3–H bonds in small molecules makes them the ideal precursors for 'late-stage functionalization' (LSF), and thus, direct C–H functionalization transformations are still a flourishing area of research.[2] Current well-established mechanistic designs for derivatizing C–H bonds include[3]: 1) deprotonation[4], 2) oxidative addition into a C–H bond via a metal catalyst[5,6], 3) insertion via a carbene or nitrene species[7-9], 4) HAT to access nucleophilic carbon-centered radicals[10-12], and lastly, 5) hydride abstraction[13-19] (Fig. 1a). The first four strategies are particularly well-developed and widespread amongst synthetic chemists.[20] In particular, HAT-based transformations in recent years have established a strong foothold in the area as a powerful approach for derivatizing C_{sp}^3–H bonds to a number of valuable functional groups. A renaissance of radical intermediates has expanded the scope of modern C–H coupling partners to include sophisticated electrophilic reagents such as SelectFluor or tosyl azide, and notably, transition-metal catalysts for coupling with abundant electrophiles such as aryl and alkyl halides.[21] In contrast, the area of hydride abstraction-based mechanisms has been slower to advance. Current methods primarily functionalize at α-heteroatom C–H sites through the use of strong Lewis acids

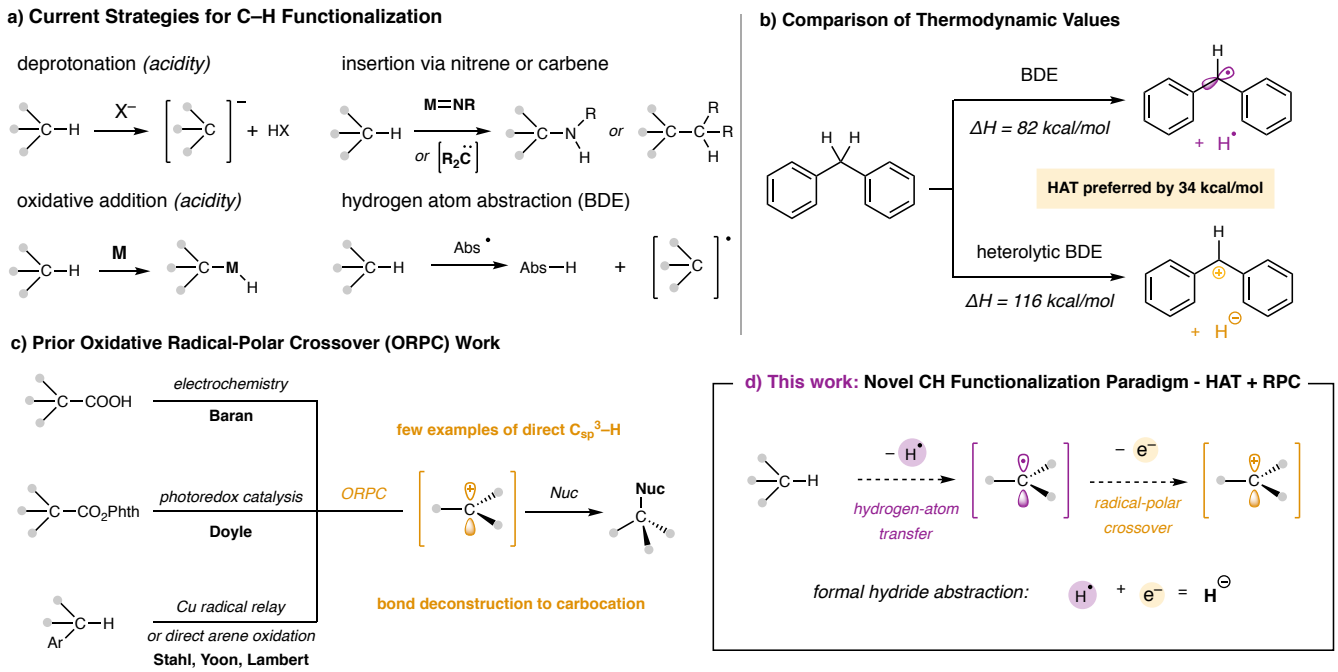

Fig. 1 | Strategies for Deconstructing C_{sp}^3–H bonds. a) Current mechanistic approaches to breaking a C_{sp}^3–H bond b) Contrasting bond dissociation energies of homolytic and heterolytic breaking events. c) Modern uses of radical-polar crossover. d) Photocatalytic HAT and RPC strategy as novel C–H functionalization platform.

to access stabilized iminium and oxocarbenium ions. Despite carbocations being reactive intermediates that have the potential to readily couple with an expansive array of nucleophilic coupling partners, which are more abundant than their electrophilic equivalents, existing hydride abstraction strategies have struggled to be generalized with respect to the C_{sp^3}–H bond. The discrepancy between HAT and hydride abstraction technologies can plausibly be rationalized by the differences in thermodynamic requirements for the two bond breaking processes. For example, the benzylic C_{sp^3}–H bond of diphenylmethane has a homolytic bond dissociation energy (BDE) of 82 kcal/mol[22], whereas its heterolytic bond dissociation energy to give a carbocation species and hydride requires 116 kcal/mol[23], a 34 kcal/mol difference (Fig. 1b).

Recently, we hypothesized that a highly reactive carbocation intermediate could be obtained from a C_{sp^3}–H bond through a stepwise mechanistic process facilitated by photoredox catalysis: a hydrogen-atom transfer (HAT) followed by a radical-polar crossover (RPC) event involving oxidation of the carbon radical to a carbocation. In recent years, radical-polar crossover has emerged as a powerful mechanistic strategy for engaging abundant inexpensive nucleophile coupling partners via the use of electrochemistry, transition-metal catalysis, and visible-light photoredox catalysis platforms (Fig. 1c). Electrochemical strategies for oxidative RPC have been utilized by the Baran group for the conversion of carboxylic acids to a number of C–heteroatom bonds.[24,25] The Doyle group recently utilized photoredox catalysis for the oxidation of carbon-centered radicals generated from phthalimide ester moieties.[26] Additionally, the groups of Chen & Xiao[27], Kim[28], Ragains[29], Zhou[30], Akita[31], Aggarwal[32], Nagib[33], and Yoon[34,35] have shown radical-cationic crossover to be an enabling element for a number of other visible light-mediated transformations. A recent publication from the groups of Song and Li combined HAT with RPC through the use of iron salts and an organophotocatalyst for a 3-component coupling strategy.[36] The use of carbocation intermediates specifically in intermolecular C–H functionalization methods is in its infancy. A radical relay strategy put forth by Stahl and coworkers, employing a copper catalyst and *N*-fluorobenzenesulfonimide (NFSI) as an oxidant, is computationally postulated to occur via a HAT–RPC sequence for the functionalization of benzylic C–H bonds with nucleophilic partners.[37-39] Net hydride removal from benzylic C_{sp^3}–H bonds has also been successfully achieved via oxidation of the adjacent

aromatic ring, with recent examples from the Yoon and Lambert laboratories, albeit under strongly oxidizing conditions.[34,40] The union of HAT with RPC to achieve a net hydride abstraction for the generation of discrete cationic species has not yet been fully realized as a general mechanistic design within the field of catalysis, despite its potential to be a highly enabling and efficient C–H functionalization platform (Fig. 1d).

We showcase the potential utility of the novel net hydride abstraction design in the area of fluorine chemistry by presenting a general C_{sp}^3–H nucleophilic fluorination methodology, followed by extension of the platform to other nucleophile classes (Fig. 2). The unique ability of fluorine to extensively alter the biological activity and metabolic stability of a drug candidate has resulted in the synthetic community placing a high value on the development of new fluorination reactions.[41-43] The prevailing mechanistic design for current robust C_{sp}^3–H fluorination strategies rely on the use of electrophilic fluorine (fluorenium) reagents[44-57], to avoid the use of fluoride as a nucleophile in the key bond-forming step, despite the many advantages they have to offer such as facile translation to radiolabeling (fluorine-18) endeavors, tunable solubility, broader functional group tolerance, comparatively lower costs, more atom economical, and possess improved safety features.[58-66] Seminal work from Groves and coworkers showcased the first demonstration of a general C_{sp}^3–H fluorination utilizing nucleophilic fluoride reagents on aliphatic substrates, albeit via an *in-situ* conversion of the fluoride to an electrophilic Mn-F species to employ a

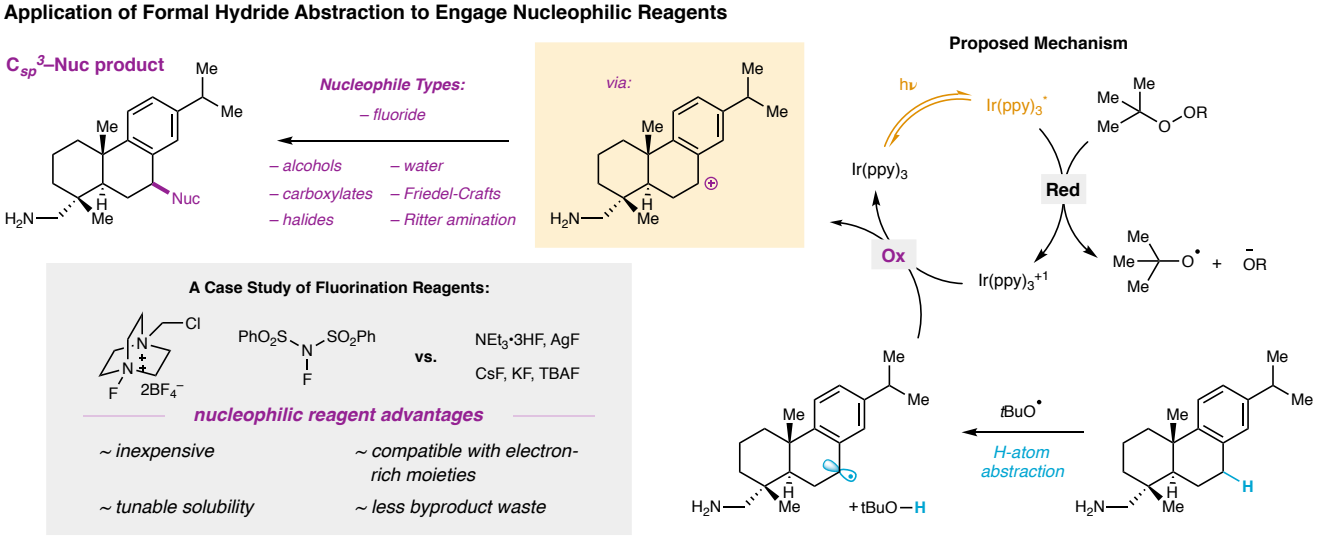

Fig. 2 | Proposed Mechanism for Formal Hydride Abstraction. Proposed hydrogen-atom abstraction coupled with radical polar crossover to access valuable carbocation intermediates for facile C–X bond formation with a variety of nucleophiles. Demonstration of the initial concept with nucleophilic fluoride sources.

radical rebound mechanism for C–F bond formation.[67,68] The paramount challenge with fluoride reagents is the weak nucleophilic reactivity they possess, thus requiring creative mechanistic strategies or new reagent discovery. Herein, we showcase the utility of the sequential HAT-RPC mechanism as a viable platform for accessing reactive carbocation intermediates under photocatalytic conditions. This mechanistic design is successful at not only engaging poor nucleophiles such as fluoride, but is also readily amenable to a plethora of other nucleophile classes that would be incompatible in radical rebound platforms. Lastly, aliphatic tertiary C_{sp^3}–H sites show potential as hydrocarbon substrates under this platform. The intermediacy of aliphatic carbocations has not been previously demonstrated by other C–H functionalization platforms that invoke key carbocation intermediates.

Reaction Design.

A critical element of the proposed formal hydride abstraction platform is the identification of an appropriate hydrogen atom abstractor that could be generated in a single-electron reduction event. Such a mechanistic element would provide a net redox neutral catalytic cycle with a visible-light photoredox catalyst. To satisfy this design principle, readily available organic peroxides that can generate known abstractor *tert*-butoxy radical (*t*BuO•)[69] were examined. Figure 2 details our proposed mechanism with such peroxide reagents. Upon visible-light excitation of a photocatalyst, single-electron reduction of an organic peroxide can lead to fragmentation of the weak O–O bond, to give alkoxy radical and alkoxide anion intermediates. H-atom abstraction of a C_{sp^3}–H bond on a hydrocarbon substrate by *t*BuO• would generate the corresponding alkyl radical, and *tert*-butanol as a benign, easily removable byproduct. Subsequent single-electron oxidation of the alkyl radical to a carbocation is proposed to occur through a single-electron transfer event with the photocatalyst. This radical-polar crossover event is quite facile, ranging from -0.11V for tertiary radicals to +0.68 V for primary (vs. SCE).[70] Generation of the carbocation in the presence of nucleophilic partners will lead to a rapid S_N1-type substitution, thereby furnishing the desired carbon-nuclephile bond.

With 1-isopropyl naphthalene as a model substrate, we tested the reductively-triggered hydrogen-atom abstractor peroxide – *tert*-butyl peroxybenzoate (TBPB, **3**) – which was gratifyingly found to work in combination with visible light, an iridium photocatalyst, $Ir(dFppy)_3$, and triethylamine-trihydrofluoride at

ambient temperature to afford 69% yield of the desired C–H fluorination product **2** (Table 1, **entry 1**). All reagents are readily available from several commercial vendors and do not require any prior preparation. The mild, noncorrosive nature of triethylamine-trihydrofluoride (TREAT-HF) has been previously documented and has played a role in the increase in selective fluorination methods.[59,71] As shown by the reduction potentials listed, TBPB is a weaker oxidant ($E_{1/2}^{red}$ = -1.38V vs SCE)[72] than common electrophilic fluorenium reagents SelectFluor and NFSI ($E_{1/2}^{red}$ = -0.33V and -1.24V vs SCE, respectively)[73]. A sufficiently reducing photocatalyst, Ir(dFppy)$_3$ ($E_{1/2}^{red}$ [Ir^{IV}/*Ir^{III}] = −1.44 V vs SCE)[74,75], is thus required and can allow for broad functional group tolerance of oxidation-sensitive moieties. Control experiments in the absence of photocatalyst and light demonstrated the dependence of the reaction on the photochemistry design element (**entries 2 and 3**). While benzene as solvent was found to provide the highest yields of fluorinated product, the reaction also proceeded in ethyl acetate or acetonitrile

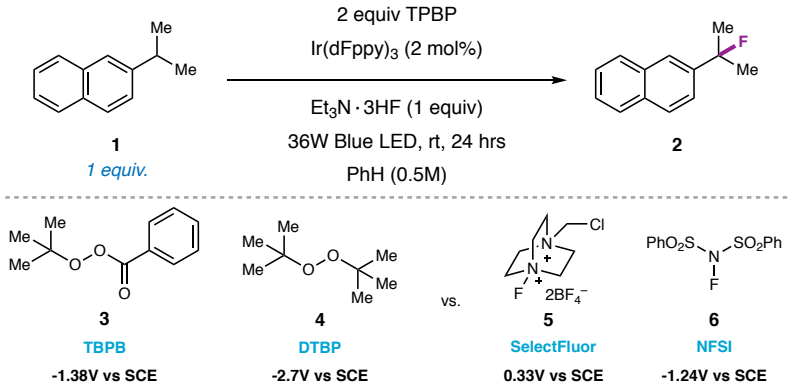

entry	deviation from standard conditions	Yield of 2[a]
1	none	69%
2	no photocatalyst	0%
3	no light	0%
4	EtOAc instead of PhH	38%
5	MeCN instead of PhH	33%
6	DTBP instead of TBPB	5%
7	BPO instead of TBPB	0%
8	CsF instead of $Et_3N \cdot 3HF$	9%
9	0.1 equiv $Et_3N \cdot 3HF$	10%

Table 1 | Optimization of Reaction and Control Studies [a] Reactions were performed on 0.20 mmol scale of the hydrocarbon. Fluorobenzene added as an external standard for determining ^{19}F NMR yields.

(**entries 4 and 5**). We hypothesize that the use of benzene assists in reducing the competitive side pathway of β-scission of the *t*BuO• radical. This fragmentation has been studied and is known to be controlled by the polarity of the solvent and concentration effects, with the rates of HAT being 2-3 orders of magnitude faster than the rate of fragmentation.[76,77] Other mild peroxides were tested but provided inferior yields compared to TBPB (**entries 6 and 7**). More basic fluoride sources were found to give lower yields (**entry 8** and see SI). Analysis of crude reaction mixtures did not detect styrene products, highlighting the propensity of the system to favor S_N1 pathways. Gratifyingly, use of the fluoride reagent in limiting quantities still results in fluorinated product, an indication that the platform could be amenable to fluorine-18 chemistry (**entry 9**).

Scope.

With a successful photoredox catalyst/peroxide system in hand, we next turned to investigating the scope of this reaction. We were delighted to find the reaction was amenable to a diverse assortment of hydrocarbon substrates (Fig. 3). Successful fluorination of cumene was observed under optimized conditions, and the presence of an electron-withdrawing group at the para position of the aryl ring was

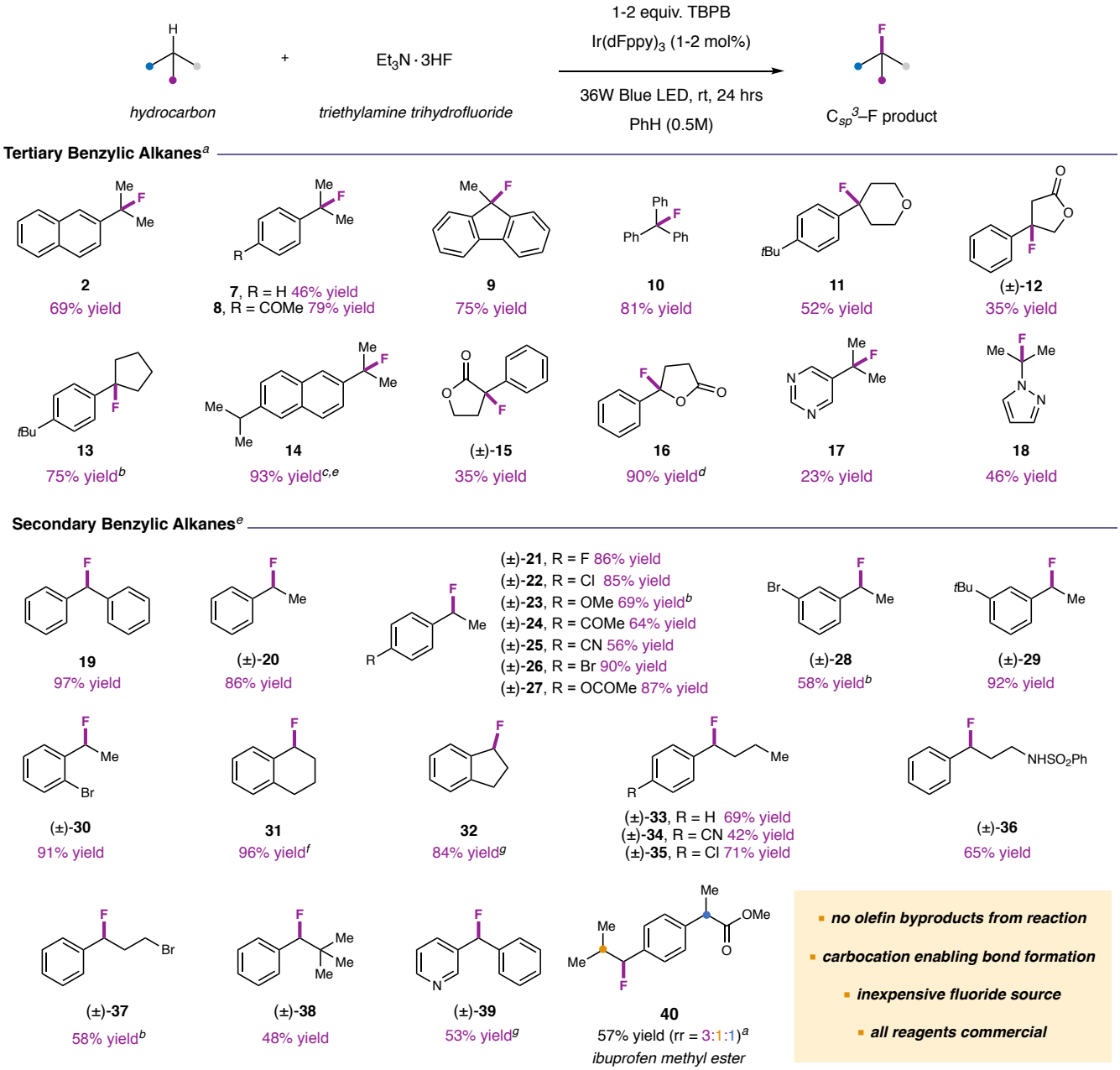

Fig. 3 | Scope of benzylic and aliphatic tertiary C–H positions. [a] C_{sp^3}–H precursor (1 equiv, 0.50 mmol), TBPB (2 equiv), Et_3N•3HF (1 equiv), benzene (0.5M), and $Ir(dFppy)_3$ (2 mol%). ^{19}F NMR yields with fluorobenzene as the external standard. [b] Reaction was run on 0.20 mmol scale. [c] 10% of difluorination product. [d] 1 equiv of TBPB with 0.66 equiv of Et_3N•3HF was used. [e] C_{sp^3}–H precursor (3 equiv, 1.50 mmol), TBPB (1 equiv, 0.5mmol), Et_3N•3HF (3 equiv, 1.5 mmol), benzene (0.5M) and $Ir(dFppy)_3$ (1 mol%). ^{19}F NMR yields. [f] Only 0.33 equiv of Et_3N•3HF was used. [g] Silver fluoride (3 equiv, 1.5 mmol) used instead of Et_3N•3HF with 1 equiv. of hydrocarbon

well-tolerated (**7, 8**). Diphenyl and triphenyl C–H positions were also viable substrates that produced excellent yields (**9, 10**). Both 5- and 6-membered rings were amenable to fluorination at benzylic positions

(**11-13**). Monofluorination was observed in high yield on a substrate with two benzylic C–H sites when used in excess with TBPB as the limiting reagent (**14**). Excitingly, benzylic sites adjacent to electron-withdrawing groups successfully provided α-fluoro products in one step, despite the challenging RPC step (**15**). A high yield was obtained for fluorination at α-oxy benzylic C–H bonds (**16**). Lastly, isopropyl-substituted heteroarenes, including pyrimidine and pyrazole, worked modestly well in the formal hydride abstraction platform (**17** and **18**).

We next turned to investigating the scope of our mechanistic platform with secondary benzylic C–H substrates. Inversion of the stoichiometry of the reaction provided good yields of monofluorinated benzylic products with TBPB as the limiting reagent. Diphenylmethane was found to work in good yield and afforded 97% yield of the monofluorinated product (**19**). Fluorination of ethylbenzene (**20**) also resulted in good yield and provided a scaffold for interrogation of substituent effects on the success of the fluorination. An examination of various electron-donating and electron-withdrawing groups on the phenyl ring found higher yields for electron-donating functionality, potentially due to the ability to better stabilize a benzylic carbocation, and thus a more facile RPC oxidation (**21-27**). The formal hydride abstraction was not deterred by meta (**28**, **29**) or ortho (**30**) substitution. Excellent yields were obtained at the benzylic position of fused 5- and 6-membered rings (**31**, **32**). For substrates containing long-chain alkyl groups, complete selectivity for the benzylic methylene position over other methylene carbons was observed, even in the case of electronically-activated α-heteroatom positions (**33-37**). Additional steric bulk with neopentyl substrate **38** saw diminished yields. Lastly, we found alkyl pyridine-based substrates could be fluorinated in modest yields upon a switch in fluoride reagent to silver fluoride (**39**). Interestingly, when triethylamine-trihydrofluoride was used as the fluoride source, 1% or less of fluorinated product was observed for these substrates, potentially offering some site selectivity opportunities on more complex substrates. For the methyl ester of Ibuprofen (**40**), fluorination at the benzylic methylene site was favored. In all substrate situations, secondary aliphatic fluorination products were undetectable.

To probe the regioselectivities of the system, a competition experiment was conducted between substrates **41** and **42** (Fig. 4). A greater than 11:1 preference for functionalization on the electron-rich substrate was observed over the electron-deficient substrate. The high regioselectivity of the reaction could potentially be utilized for site selectivity on more complex systems. Substrates **43** and **45** contain secondary benzylic, aliphatic tertiary, and secondary and primary C_{sp}^3–H bonds. Upon treatment with the standard reaction conditions, both substrates were preferentially fluorinated at the secondary benzylic position in >2:1 ratio relative to the tertiary aliphatic site in high yield.

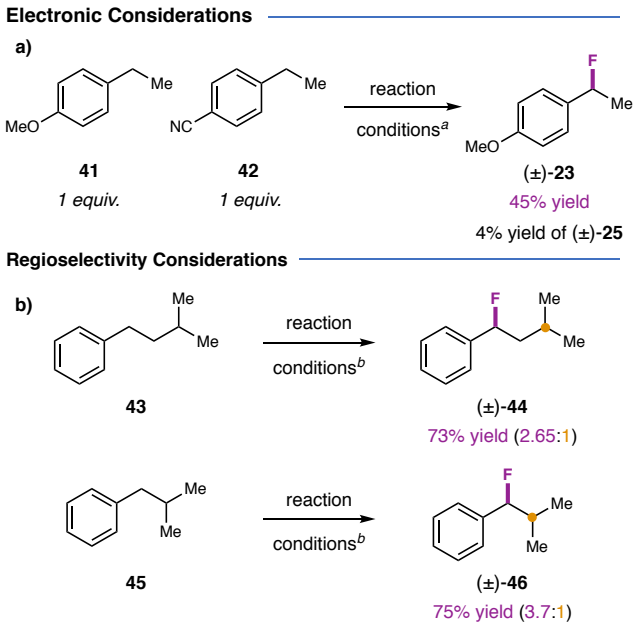

Fig. 4 | *Regioselectivity of the Formal Hydride Abstraction.* *a) Electronic Considerations. [a] Reaction conditions: C_{sp}^3–H precursors (0.2 mmol, 1 equiv), TBPB (2 equiv), Et_3N•3HF (1 equiv), $Ir(dFppy)_3$ (2 mol%) and benzene (0.5M). ^{19}F NMR yields. b) Regioselectivity Considerations. [b] Reaction conditions: C_{sp}^3–H precursors (3 equiv), TBPB (0.2 mmol 1 equiv), Et_3N•3HF (3 equiv), and $Ir(dFppy)_3$ (2 mol%) and benzene (0.5M). ^{19}F NMR yields.*

Precursors containing aliphatic C–H sites were evaluated next. Aliphatic C_{sp}^3–H bonds represent a more uphill hydride abstraction than benzylic positions, with the cited heterolytic BDE being 234 kcal/mol[78] for isobutane, compared to a homolytic BDE value of 100 kcal/mol. We were elated to observe that the formal hydride abstraction design successfully functionalized the tertiary position of adamantane in 18% yield (Fig. 5, **47**). Notably, no 2-fluoroadamantane product (**48**) was detected, indicating the method is wholly selective for 3º aliphatic positions over 2º. As such, our system offers complementary utility to the Mn-catalyzed conditions by Groves and coworkers. While the Mn-catalyzed conditions provide greater yields of fluorinated material, poorer selectivity between the two sites was achieved due to the ability to abstract from both 3º and 2º aliphatic positions.[67] The divergent nature of our HAT-RPC protocol and Groves's HAT-coordination method is further exemplified by the results of attempted fluorination of diterpene amine natural product leelamine (**49**), bearing a primary amine. Under our formal hydride abstraction conditions, 41% yield of fluorinated product is observed, with 4:1 selectivity for the

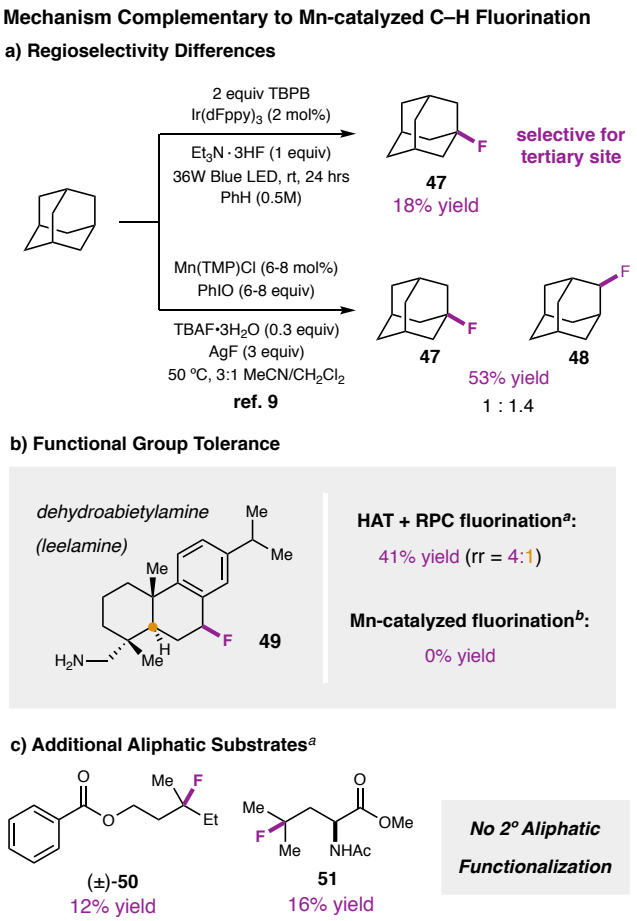

Fig. 5 | Complementary selectivity and reactivity to Mn-catalyzed C–H Fluorination. a) Regioselectivity differences between 3º and 2º aliphatic sites. b) Divergent functional group tolerance for substrates containing basic sites. [a] leelamine (0.5 mmol, 1 equiv), TBPB (2 equiv), Et_3N•3HF (1 equiv), $Ir(dFppy)_3$ (2 mol%) and benzene (0.5M). ^{19}F NMR yields. [b] leelamine (0.2 mmol, 1 equiv), Et_3N•3HF (1.5 equiv), iodosylbenzene (9 equiv) Mn(salen)Cl (20 mol%), MeCN at 50 °C. See reference 79. c) Additional 3º aliphatic fluorination.

cyclic secondary benzylic position. In contrast, Groves's method, which relies upon fluoride coordination at a Mn center, is wholly unsuccessful at functionalizing leelamine, potentially due to the competitive coordinating abilities of the primary amine.[79] Lastly, long-chain aliphatic substrate **50** also afforded fluorinated product in 12% yield selectively at the tertiary position, again with no detection of secondary aliphatic C–H fluorination. Fluorination of leucine was also successful, highlighting possibilities of this reactivity platform on amino acids for protein modification applications (**51**).

Next, we questioned whether or not difluorination products could be accessed directly from benzylic methylene substrates, which possess two abstractable C_{sp^3}–H bonds at the benzylic position. The importance of difluoromethylene groups (CF_2) in medicinal chemistry scaffolds has received recent attention due to their numerous benefits in drug design, such as locked substrate conformations, alcohol, sulfone, and sulfamide isosteres, modulation of basicity and dipole moments, and increased metabolic stability.[80] We envision that our stepwise hydride abstraction design could be utilized to achieve an *in-situ* double formal hydride abstraction via a sequential abstraction on the monofluorinated product that would involve the intermediacy of an α-fluoro carbocation (Fig. 6). Classically, α-fluoro carbocations are generated either through the nucleophilic nature of a vinyl fluoride moiety, a strong Lewis acid association to a multifluorinated substrate, or the use of fluoro oxidants, and have been ideal intermediates for access to a plethora of alternative organofluorine compounds.[81,82] This

stepwise formal hydride abstraction paradigm could offer a C–H functionalization strategy to directly accessing valuable α-fluoro carbocation species from methylene sites under mild conditions. Excitingly, difluoromethylene products were observed when the hydrocarbon precursor was employed as the limiting reagent with excess fluoride and hydrogen-atom abstractor. Difluorination of diphenylmethane worked well, providing 55% yield of **19'**. High yields of **19'** were also achieved when compound **19** was

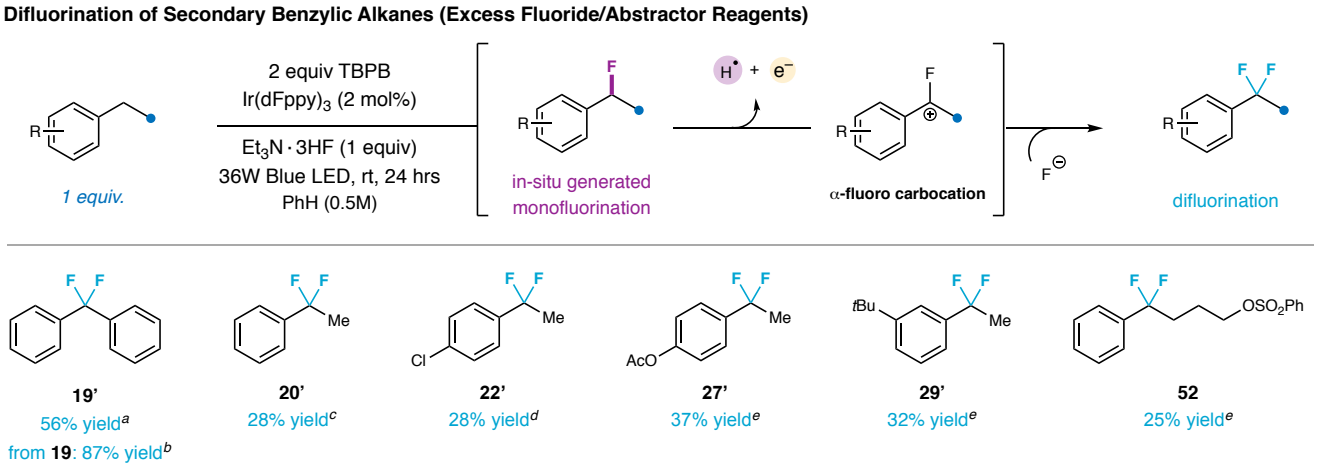

Fig. 6 | Difluorination of secondary benzylic alkanes. Reaction conditions: C_{sp^3}–H precursor (1 equiv, 0.50 mmol), TBPB (2 equiv), Et_3N•3HF (1 equiv), benzene (0.5M), and $Ir(dFppy)_3$ (2 mol%). ^{19}F NMR yields. [a] 32% of **23** [b] Compound **19** was utilized as the substrate instead of diphenylmethane [c] 41% of **20** [d] 50% of **22** [e] 55-58% yield of **27, 29**, and monofluoro product of **52**.

subjected to the nucleophilic fluorination conditions. We were encouraged to observe difluoromethylene products of ethylbenzene scaffolds (**20', 22', 27'**). Meta substitution was tolerated (**29'**), while ortho substitution shut down the difluorination (See SI). Additional length in the alkyl chain of secondary benzylic substrates was tolerated for the difluorination (**52**). While high yielding methylene difluorination has been reported by Chen and coworkers,[51] to the best of our knowledge, this represents the first example with nucleophilic fluoride.

Next, we considered the identity of the electrophilic hydrogen atom abstractor (Fig. 7a). While we hypothesize TBPB fragments upon SET reduction to provide tBuO• and benzoate, recent work by Glorius and co-workers demonstrates that benzoxy radical, •OCOPh, could also be a viable catalytic H-atom abstractor species.[83] Thus, Figure 7a shows two possible fragmentation pathways of the perester upon reduction. In order to interrogate pathway 1 vs. pathway 2, we tested symmetrical peroxide benzoyl peroxide (BPO), which fragments to give benzoxy radical and benzoate anion, under our reaction conditions. No fluorination product was observed with BPO, suggestion the benzoxy radical is unlikely to be a HAT catalyst under our reaction conditions. Next, di-*tert*-butyl peroxide (DTBP) was investigated as

the peroxide, which provided only 5% yield of the fluorinated product. Stern-Volmer experiments showed relatively weak quenching of the photocatalyst in the presence of DTBP, which suggests the lack of success of DTBP may be due to a high reduction potential (-2.7V v SCE)[84] that is not within the reducing ability of the photocatalyst. Conversely, TBPB efficiently quenched the photocatalyst.[85] Together, this data suggests the identity of the hydrogen atom abstractor to be *t*BuO• (pathway 1).

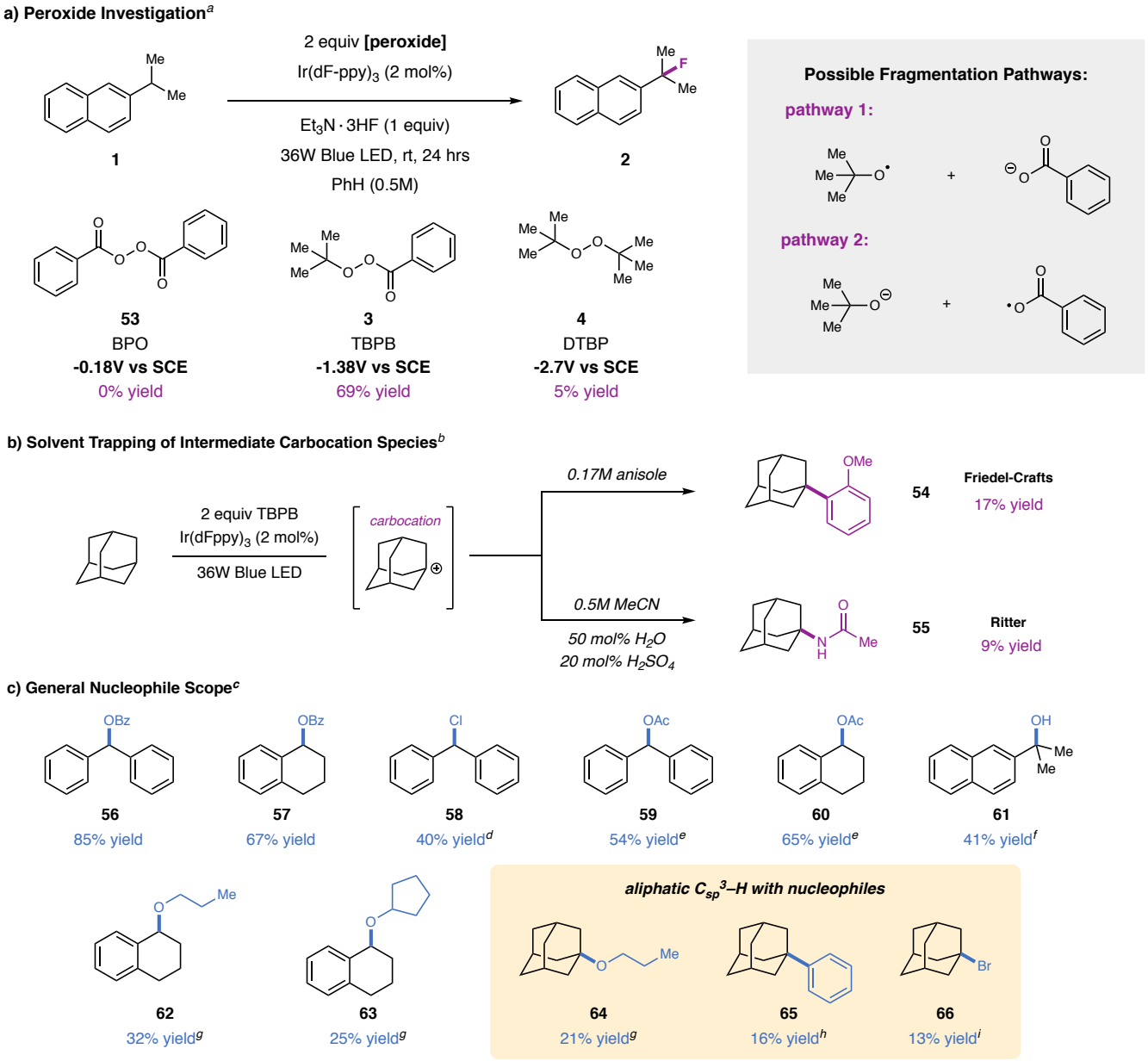

Fig. 7 | Further considerations and alternative nucleophiles in formal hydride abstraction platform. a) Peroxide Investigation. [a] Reaction was run on 0.20 mmol scale. b) Solvent trapping of intermediate carbocation species. [b] Reaction was run on 0.50 mmol scale. Isolated yields. c) General nucleophile scope. [c] Reaction conditions: $C_{sp}{}^3$–H precursor (5 equiv, 2.50 mmol), TBPB (1 equiv, 0.5mmol), benzene (0.5M) and $Ir(dFppy)_3$ (2 mol%) with isolated yields. [d] 1 equiv of TBACl = tetrabutylammonium chloride was used. ^{1}H NMR yield with mesitylene as the external standard. [e] TBEC was used instead of TBPB with 1 equiv of acetic acid and 10 equiv. of hydrocarbon [f] 1:1 H_2O:MeCN solvent was used with 1 equiv. tetraline and 2 equiv TBPB [g] 1 equiv of tetraline substrate was used with 5 equiv alcohol reagent, 1.2 equiv TBPB, and 0.2M dichloroethane. ^{1}H NMR yield for **64**, [h] 1 equiv of adamantane was employed and TBEC was used instead of TBPB h [i] 1 equiv of adamantane was employed with 3 equiv of TBAB = tetrabutylammonium bromide in benzene (0.17M). ^{1}H NMR yield.

To probe the intermediacy of a reactive carbocation species, we attempted to trap out the carbocation with classical carbocation reaction partners (Fig. 7b). Replacement of the reaction solvent with anisole and removal of the fluoride reagent led to the isolation of a Friedel-Crafts product (**54**). Additionally, use of aqueous acetonitrile as the solvent system revealed Ritter product **55**. Such products are unlikely to arise from solely a carbon-centered radical intermediate. With these results in hand, we turned to investigate the potential of the photocatalytic hydride abstraction to incorporate other classes of nucleophiles (Fig. 7c). Gratifying, the HAT-RPC protocol was amenable to coupling a wide array of nucleophiles with a number of different C_{sp^3}–H bonds. Benzoate compounds **56** and **57** demonstrate the ability of TBPB to provide dual functionality as both the abstractor source and the nucleophile. Chlorination was also possible with the use of tetrabutylammonium chloride (**58**). Acetoxylation with acetic acid was achieved for both diphenylmethane and tetraline hydrocarbon (**59** and **60**) via employment of commercially available *tert*-butylperoxy 2-ethyhexyl carbonate (TBEC) as the peroxide rather than TBPB so as to avoid benzoate-coupled products. When a 1:1 H_2O:MeCN solvent mixture was employed, tertiary alcohol **61** was isolated, representing a C–H hydroxylation strategy with water. Excitingly, propanol and cyclopentanol were also viable nucleophiles for the reaction platform, demonstrating its potential for etherification, albeit in diminished yields (**62** and **63**). Aliphatic tertiary C–H sites on adamantane also coupled with an alcohol, arene and halide nucleophile under the photocatalytic conditions. Substrates **64**, **65** and **66** represent a class of hydrocarbon substrates not viable in other carbocation-employing C_{sp^3}–H functionalization strategies, which have only demonstrated derivatization of benzylic C–H sites.

In summation, photoredox catalysis can be utilized to access highly reactive carbocations directly from C_{sp^3}–H bonds under mild conditions without paying the high energetic penalty required for a direct heterolytic bond cleavage. We have successfully identified a reaction platform that acts as a formal hydride abstraction surrogate through the combination of two elementary

steps – HAT followed by a radical-cationic crossover. The broadly applicable platform utilizes all commercially-available reagents in conjunction with visible-light photoredox catalysis, thus providing mild and easy-to-use conditions. We have demonstrated the initial success of the novel C_{sp^3}–H functionalization platform in the realm of C–H fluorination, specifically leveraging the platform to take advantage of the benefits of nucleophilic fluoride sources. In addition, we have also successfully demonstrated the interception of the carbocation intermediate by other nucleophile classes, furthering the potential impact of this formal hydride abstraction on practicing chemists.

References

1. Abrams, D. J., Provencher, P. A. & Sorensen, E. J. Recent applications of C-H functionalization in complex natural product synthesis. *Chem. Soc. Rev.* **47**, 8925–8967 (2018).
2. Govaerts, S., Nyuchev, A. & Noel, T. Pushing the boundaries of C–H bond functionalization chemistry using flow technology. *J. of Flow Chem.* **10**, 13–71 (2020).
3. Roudesly, F., Oble, J. & Poli, G. Metal-catalyzed C–H activation/functionalization: The fundamentals. *J. Mol. Catal. A Chem.* **426**, 275–296 (2017).
4. Bergman, R. G. C – H activation. *Nature* **446**, 391-394. (2007).
5. Wencel-Delord, J., Dröge, T., Liu, F. & Glorius, F. Towards mild metal-catalyzed C–H bond activation. *Chem. Soc. Rev.* **40**, 4740–4761 (2011).
6. Goldman, A. S. & Goldberg, K. I. Organometallic C—H Bond Activation: An Introduction. **14**, 1–43 (UTC, 2004).
7. Davies, H. M. L. & Manning, J. R. Catalytic C-H functionalization by metal carbenoid and nitrenoid insertion. *Nature* **451**, 417–424 (2008).
8. Doyle, M. P., Duffy, R., Ratnikov, M. & Zhou, L. Catalytic carbene insertion into C-H bonds. *Chem. Rev.* **110**, 704–724 (2010).
9. Díaz-Requejo, M. M. & Pérez, P. J. Coinage metal catalyzed C - H bond functionalization of hydrocarbons. *Chem. Rev.* **108**, 3379–3394 (2008).
10. Stateman, L. M., Nakafuku, K. M. & Nagib, D. A. Remote C–H Functionalization via Selective Hydrogen Atom Transfer. *Synthesis* **50**, 1569–1586 (2018).
11. Capaldo, L. & Ravelli, D. Hydrogen Atom Transfer (HAT): A Versatile Strategy for Substrate Activation in Photocatalyzed Organic Synthesis. *Euro. J. Org. Chem.* **2017**, 2056–2071 (2017).
12. Capaldo, L., Quadri, L. L. & Ravelli, D. Photocatalytic hydrogen atom transfer: The philosopher's stone for late-stage functionalization? *Green Chemistry* **22**, 3376–3396 (2020).
13. Basak, S., Winfrey, L., Kustiana, B. A., Melen, R. L., Morrill, L. C. & Pulis, A. P. Electron deficient borane-mediated hydride abstraction in amines: stoichiometric and catalytic processes. *Chem. Soc. Rev.* **50**, 3720-3737 (2021).
14. Davies, H. M. L. & Morton, D. Recent Advances in C-H Functionalization. *J. Org. Chem.* **81**, 343–350 (2016).
15. Chen, W., Paul, A., Abboud, K. A. & Seidel, D. Rapid functionalization of multiple C–H bonds in unprotected alicyclic amines. *Nat. Chem.* **12**, 545–550 (2020).
16. Mori, K., Kurihara, K., Yabe, S., Yamanaka, M. & Akiyama, T. Double C(sp^3)-H Bond Functionalization Mediated by Sequential Hydride Shift/Cyclization Process: Diastereoselective Construction of Polyheterocycles. *J. Am. Chem. Soc.* **136**, 3744–3747 (2014).
17. Basak, S., Alvarez-Montoya, A., Winfrey, L., Melen, R. L., Morrill, L. C. & Pulis, A. P. $B(C_6F_5)_3$-Catalyzed

Direct C3 Alkylation of Indoles and Oxindoles. *ACS Catal.* **10**, 4835–4840 (2020).
18. Chan, J. Z., Yesilcimen, A., Cao, M., Zhang, Y., Zhang, B. & Wasa, M. Direct Conversion of N-Alkylamines to N-Propargylamines through C-H Activation Promoted by Lewis Acid/Organocopper Catalysis: Application to Late-Stage Functionalization of Bioactive Molecules. *J. Am. Chem. Soc.* **142**, 16493–16505 (2020).
19. Wang, T., Wang, L., Daniliuc, C. G., Samigullin, K., Wagner, M., Kehr, G. & Erker, G. CO/CO and NO/NO coupling at a hidden frustrated Lewis pair template. *Chem. Sci.* **8**, 2457–2463 (2017).
20. Chu, J. C. K. & Rovis, T. Complementary Strategies for Directed C(sp3)−H Functionalization: A Comparison of Transition-Metal-Catalyzed Activation, Hydrogen Atom Transfer, and Carbene/Nitrene Transfer. *Angew. Chem. Int. Ed.* **57**, 62–101 (2018).
21. Shaw, M. H., Twilton, J. & MacMillan, D. W. C. Photoredox Catalysis in Organic Chemistry. *J. Org. Chem.* **81**, 6898-6926 (2016).
22. Luo, Y. R. *Handbook of bond dissociation energies in organic compounds*, 1st ed.; CRC Press, 2002.
23. Ilic, S.; Alherz, A.; Musgrave, C. B. & Glusac, K. D. Thermodynamic and kinetic hydricities of metal-free hydrides. *Chem. Soc. Rev.* **47**, 2809–2836 (2018).
24. Xiang, J., Shang, M., Kawamata, Y., Lundberg, H., Reisberg, S. H., Chen, M., Mykhailiuk, P., Beutner, G., Collins, M. R., Davies, A., Del Bel, M., Gallego, G. M., Spangler, J. E., Starr, J., Yang, S., Blackmond, D. G. & Baran, P. S. Hindered dialkyl ether synthesis with electrogenerated carbocations. *Nature* **573**, 398-402 (2019).
25. Sheng, T., Zhang, H.-J., Shang, M., He, C., Vantourout, J. C. & Baran, P. S. Electrochemical Decarboxylative *N*-Alkylation of Heterocycles *Org. Lett.* **22**, 7594–7598 (2020).
26. Webb, E. W., Park, J. B., Cole, E. L., Donnelly, D. J., Bonacorsi, S. J., Ewing, W. R. & Doyle, A. G. Nucleophilic (Radio)Fluorination of Redox-Active Esters via Radical-Polar Crossover Enabled by Photoredox Catalysis. *J. Am. Chem. Soc.* **142**, 9493–9500 (2020).
27. Guo, W., Cheng, H.-G., Chen, L.-Y., Xuan, J., Feng, Z.-J., Chen, J.-R., Lu, L.-Q. & Xiao, W.-J. *De Novo* Synthesis of γ,γ-Disubstituted Butyrolactones through a Visible Light Photocatalytic Arylation-Lactonization Sequence. *Adv. Synth. Catal.* **356**, 2787–2793 (2014).
28. Kwon, S. J. & Kim, D. Y. Visible Light Photoredox-Catalyzed Arylative Ring Expansion of 1-(1-Arylvinyl)cyclobutanol Derivatives. *Org. Lett.* **18**, 4562–4565 (2016).
29. Hollister, K. A., Conner, E. S., Spell, M. L., Deveaux, K., Maneval, L., Beal, M. W. & Ragains, J. R. Remote Hydroxylation through Radical Translocation and Polar Crossover. *Angew. Chem. Int. Ed.* **54**, 7837–7841 (2015).
30. Li, L., Chen, H., Mei, M. & Zhou, L. Visible-light promoted γ-cyanoalkyl radical generation: three-component cyanopropylation/etherification of unactivated alkenes. *Chem. Commun.* **53**, 11544–11547 (2017).
31. Nakayama, Y., Ando, G., Abe, M., Koike, T. & Akita, M. Keto-Difluoromethylation of Aromatic Alkenes by Photoredox Catalysis: Step-Economical Synthesis of α-CF_2H-Substituted Ketones in Flow. *ACS Catal.* **9**, 6555–6563 (2019).
32. Silvi, M., Sandford, C. & Aggarwal, V. K. Merging Photoredox with 1,2-Metallate Rearrangements: The Photochemical Alkylation of Vinyl Boronate Complexes. *J. Am. Chem. Soc.* **139**, 5736–5739 (2017).
33. Prusinowski, A. F., Twumasi, R. K., Wappes, E. A. & Nagib, D. A. *Vicinal*, Double C−H Functionalization of Alcohols via an Imidate Radical-Polar Crossover Cascade. *J. Am. Chem. Soc.* **142**, 5429-5438 (2020).
34. Lee, B. J., DeGlopper, K. S. & Yoon, T. P. Site-Selective Alkoxylation of Benzylic C–H Bonds by Photoredox Catalysis. *Angew. Chem. Int. Ed.* **59**, 197-202 (2020).
35. Reed, N. L., Lutovsky, G. A. & Yoon, T. P. Copper-Mediated Radical-Polar Crossover Enables Photocatalytic Oxidative Functionalization of Sterically Bulky Alkenes. *J. Am. Chem. Soc.* doi.org/10.1021/jacs.1c02747 (2021).
36. Ouyang, X. H., Li, Y., Song, R. J., Hu, M., Luo, S. & Li, J. H. Intermolecular dialkylation of alkenes with two distinct C(sp^3)H bonds enabled by synergistic photoredox catalysis and iron catalysis. *Sci. Adv.* **5**, eaav9839 (2019).
37. Zhang, W., Wang, F., McCann, S. D., Wang, D., Chen, P., Stahl, S. S. & Liu, G. Enantioselective cyanation of benzylic C–H bonds via copper-catalyzed radical relay. *Science* **353**, 1014-1018 (2016).
38. Suh, S.-E., Chen, S.-J., Mandal, M., Guzei, I. A., Cramer, C. J. & Stahl, S. S. Site-Selective Copper-Catalyzed Azidation of Benzylic C–H Bonds. *J. Am. Chem. Soc.* **142**, 11388–11393 (2020).
39. Hu, H., Chen, S.-J., Mandal, M. Pratik, S. M., Buss, J. A., Krska, S. W., Cramer, C. J. & Stahl, S. S. Copper-catalysed benzylic C–H coupling with alcohols via radical relay enabled by redox buffering. *Nat. Catal.* **3**,

358–367 (2020).
40. Shen, T. & Lambert, T. H. Electrophotocatalytic diamination of vincinal C–H bonds. *Science* **371**, 620-626 (2021).
41. Gillis, E. P., Eastman, K. J., Hill, M. D., Donnelly, D. J. & Meanwell, N. A. Applications of Fluorine in Medicinal Chemistry. *J. Med. Chem.* **58**, 8315–8359 (2015).
42. Purser, S., Moore, P. R., Swallow, S. & Gouverneur, V. Fluorine in medicinal chemistry. *Chem. Soc. Rev.* **37**, 320–330 (2008).
43. Wang, J., Sánchez-Roselló, M., Aceña, J. L., del Pozo, C., Sorochinsky, A. E., Fustero, S., Soloshonok, V. A. & Liu, H. Fluorine in Pharmaceutical Industry: Fluorine-Containing Drugs Introduced to the Market in the Last Decade (2001-2011). *Chem. Rev.* **114**, 2432–2506 (2014).
44. Neumann, C. N. & Ritter, T. Late-Stage Fluorination: Fancy Novelty or Useful Tool? *Angew. Chem. Int. Ed.* **54**, 3216-3221 (2015).
45. Szpera, R., Moseley, D. F. J., Smith, L. B., Sterling, A. J. & Gouverneur, V. The Fluorination of C−H Bonds: Developments and Perspectives. *Angew. Chem. Int. Ed.* **58**, 14824–14848 (2019).
46. Furuya, T., Kamlet, A. S. & Ritter, T. Catalysis for fluorination and trifluoromethylation. *Nature* **473**, 470–477 (2011).
47. Bloom, S., Pitts, C. R., Miller, D. C., Haselton, N., Holl, M. G., Urheim, E. & Lectka, T. A Polycomponent Metal-Catalyzed Aliphatic, Allylic, and Benzylic Fluorination. *Angew. Chem. Int. Ed.* **51**, 10580-10583 (2012).
48. Bloom, S., Pitts, C. R., Woltornist, R., Griswold, A., Holl, M. G. & Lectka, T. Iron(II)-Catalyzed Benzylic Fluorination *Org. Lett.* **15**, 1722-1724 (2013).
49. Bloom, S., Sharber, S. A., Holl, M. G., Knippel, J. L. & Lectka, T. Metal-Catalyzed Benzylic Fluorination as a Synthetic Equivalent to 1,4-Conjugate Addition of Fluoride *J. Org. Chem.* **78**, 11082-11086 (2013).
50. Bloom, S., Knippel, J. L. & Lectka, T. A photocatalyzed aliphatic fluorination. *Chem. Sci.* **5**, 1175-1178 (2014).
51. Xia, J.-B., Zhu, C. & Chen, C. Visible Light-Promoted Metal-Free C−H Activation: Diarylketone Catalyzed Selective Benzylic Mono- and Difluorination. *J. Am. Chem. Soc.* **135**, 17494-17500 (2013).
52. Xia, J.-B., Zhu, C. & Chen, C. Visible light-promoted metal-free sp^3-C–H fluorination. *Chem. Commun.* **50**, 11701-11704 (2014).
53. Halperin, S. D., Fan, H., Chang, S., Martin, R. E. & Britton, R. A Convenient Photocatalytic Fluorination of Unactivated C–H Bonds. *Angew. Chem. Int. Ed.* **53**, 4690-4693 (2014).
54. Halperin, S. D., Kwon, D., Holmes, M., Regalado, E. L., Campeau, L.-C., DiRocco, D. A. & Britton, R. Development of a Direct Photocatalytic C−H Fluorination for the Preparative Synthesis of Odanacatib. *Org. Lett.* **17**, 5200-5203 (2015).
55. Nodwell, M. B., Bagai, A., Halperin, S. D., Martin, R. E., Knust, H. & Britton, R. Direct photocatalytic fluorination of benzylic C–H bonds with N-fluorobenzenesulfonimide. *Chem. Commun.* **51**, 11783-11786 (2015).
56. Meanwell, M., Nodwell, M., Martin, R. E. & Britton, R. A Convenient Late-Stage Fluorination of Pyridylic C−H Bonds with *N*-Fluorobenzenesulfonimide. *Angew. Chem. Int. Ed.* **55**, 13244-13248 (2016).
57. Vasilopoulous, A., Golden, D. L., Buss, J. A. & Stahl, S. S. Copper-Catalyzed C–H Fluorination/Functionalization Sequence Enabling Benzylic C–H Cross Coupling with Diverse Nucleophiles. *Org. Lett.* **22**, 5753-5757 (2020).
58. Lin, A., Huehls, C. B. & Yang, J. Recent advances in C–H fluorination. *Org. Chem. Front.* **1**, 434-438 (2014).
59. Liang, S., Hammond, G. B. & Xu, B. Hydrogen Bonding: Regulator for Nucleophilic Fluorination. *Chem. Eur. J.* **23**, 17850-17861 (2017).
60. Wu, J. Review of recent advances in nucleophilic C–F bond-forming reactions at sp^3 centers. *Tetrahedron Lett.* **55**, 4289-4294 (2014).
61. McMurtrey, K. B., Racowski, J. M. & Sanford, M. S. Pd-Catalyzed C–H Fluorination with Nucleophilic Fluoride. *Org. Lett.* **14**, 4094-4097 (2012).
62. Sorlin, A. M., Usman, F. O., English, C. K. & Nguyen, H. M. Advances in Nucleophilic Allylic Fluorination. *ACS Catal.* **10**, 11980-12010 (2020).
63. Hollingworth, C. & Gouverneur, V. Transition metal catalysis and nucleophilic fluorination. *Chem. Commun.* **48**, 2929-2942 (2012).
64. McPake, C. B. & Sanford, G. Selective Continuous Flow Processes Using Fluorine Gas. *Org. Process Res. Dev.* **16**, 844-851 (2012).

65. Liang, T., Neumann, C. N. & Ritter, T. Introduction of Fluorine and Fluorine-Containing Functional Groups. *Angew. Chem. Int. Ed.* **52**, 8214-8264 (2013).
66. Braun, M.-G. & Doyle, A. G. Palladium-Catalyzed Allylic C–H Fluorination. *J. Am. Chem. Soc.* **135**, 12990-12993 (2013).
67. Liu, W., Huang, X., Cheng, M.-J., Nielsen, R. J., Goddard III, W. A. & Groves, J. T. Oxidative Aliphatic C-H Fluorination with Fluoride Ion Catalyzed by a Manganese Porphyrin. *Science* **337**, 1322-1325 (2012).
68. Liu, W. & Groves, J. T. Manganese-Catalyzed Oxidative Benzylic C–H Fluorination by Fluoride Ions. *Angew. Chem. Int. Ed.* **52**, 6024-6027 (2013).
69. Finn, M., Friedline, R., Suleman, N. K., Wohl, C. J. & Tanko, J. M. Chemistry of the t-butoxyl radical: Evidence that most hydrogen abstractions from carbon are entropy-controlled. *J. Am. Chem. Soc.* **126**, 7578–7584 (2004).
70. Fu, Y., Liu, L., Yu, H. Z., Wang, Y. M. & Guo, Q. X. Quantum-chemical predictions of absolute standard redox potentials of diverse organic molecules and free radicals in acetonitrile. *J. Am. Chem. Soc.* **127**, 7227–7234 (2005).
71. Haufe, G. Triethylamine Trishydrofluoride in Synthesis. *J. prakt. Chem.* **338**, 99-113 (1996).
72. Baron, R., Darchen, A. & Hauchard, D. Electrode reaction mechanisms for the reduction of *tert*-butyl peracetate, lauryl peroxide and dibenzoyl peroxide. *Electrochim. Acta* **51**, 1336–1341 (2006).
73. Girina, G. P., Fainzil'berg, A. A. & Feoktistov, L. G. Reduction potential as a measure of activity of the N-F fluorinating agents. *Russian Journal of Electrochemistry* **36**, 162–163 (2000).
74. Tian, N., Lenkeit, D., Pelz, S., Fischer, L. H., Escudero, D., Schiewek, R., Klink, D., Schmitz, O. J., Gonzalez, L., Schaferling, M. & Holder, E. Structure–Property Relationship of Red- and Green-Emitting Iridium(III) Complexes with Respect to Their Temperature and Oxygen Sensitivity. *Eur. J. Inorg. Chem.* **30**, 4875-4885 (2010).
75. Koike, T. & Akita, M. Visible-light radical reaction designed by Ru- and Ir-based photoredox catalysis. *Inorg. Chem. Front.* **1**, 562 (2014).
76. Avila D. V., Brown C. E., Ingold K. U. & Lusztyk J. Solvent effects on the competitive .beta.-scission and hydrogen atom abstraction reactions of the cumyloxyl radical. Resolution of a long-standing problem *J Am Chem Soc*. **115**, 466-470 (1993).
77. Walling C. & Wagner P. J. Positive Halogen Compounds. X. Solvent Effects in the Reactions of t-Butoxy Radicals *J Am Chem Soc*. **86**, 3368-3375 (1964).
78. Screttas, C. G. Some Properties of Heterolytic Bond Dissociation Energies and Their Use as Molecular Parameters for Rationalizing or Predicting Reactivity. *J. Org. Chem.* **45**, 333–336 (1980).
79. Reaction was run with 20 mol% Mn(salen)Cl and 9 equiv of PhIO catalyst according to the following: Liu, W., Huang, X. & Groves. J. T. Oxidative aliphatic C–H fluorination with manganese catalysts and fluoride ion. *Nat. Protoc* **8**, 2348-2354 (2013). Control reactions were performed to verify accuracy of the reaction in our hands. Reaction details are provided in the SI.
80. Carvalho, D. R. & Christian, A. H. Modern approaches towards the synthesis of geminal difluoroalkyl groups. *Org. Biomol. Chem.* **19**, 947-964 (2021).
81. Krespan, C. G. & Petrov, V. A. The Chemistry of Highly Fluorinated Carbocations. *Chem. Rev.* **96**, 3269–3301 (1996).
82. Ni, C. & Hu, J. The unique fluorine effects in organic reactions: Recent facts and insights into fluoroalkylations. *Chem. Soc. Rev.* **45**, 5441–5454 (2016).
83. Mukherjee, S., Maji, B., Tlahuext-Aca, A. & Glorius, F. Visible-Light-Promoted Activation of Unactivated C(sp^3)-H Bonds and Their Selective Trifluoromethylthiolation. *J. Am. Chem. Soc.* **138**, 16200–16203 (2016).
84. Donkers, R. L., Maran, F., Wayner, D. D. M. & Workentin, M. S. Kinetics of the reduction of dialkyl peroxides. New insights into the dynamics of dissociative electron transfer. *J. Am. Chem. Soc.* **121**, 7239–7248 (1999).
85. See SI for Stern-Volmer details.

Acknowledgements

The authors would like to thank B. Adams and W. Massefski from MIT DCIF, as well as A. Ali and C. Schiffer from UMass Medical School for assistance with ^{19}F NMR. The authors would also like to thank C. C. Le, J. M. Lipshultz, and E. R. Welin for their assistance in preparing the manuscript. Lastly, the authors would like to thank A. G. Doyle, I. N.-M. L., M. A. Tekle-Smith for sharing results before publication.

Author contributions

P.Z.M. and Y.Z. conceived of the work; Y.Z., I.B., and P.Z.M. conducted initial optimization; N.A.F. synthesized precursors; Y.Z. performed all fluorination experiments; N.A.F. and M.D. performed the experiments in the non-fluoride nucleophiles table; Y.Z. and P.Z.M conducted the mechanistic experiments; H.G.Y. and M.L. consulted on the substrate scope, context of the chemistry, and preparation of the manuscript; P.Z.M. prepared the manuscript with input from all coauthors.

Competing interests

The authors declare no competing interests.

Additional information

Supporting Information The Supporting Information is available free of charge. PDF includes descriptions of experiments and spectral data.

Author Information Reprints and permissions information is available at www.nature.com/reprints. Correspondence and requests for materials should be addressed to P.Z.M. (pzmusacchio@wpi.edu).

Funding Sources

Research reported in this publication was supported by a startup grant from Worcester Polytechnic Institute and resources from Pfizer Inc.
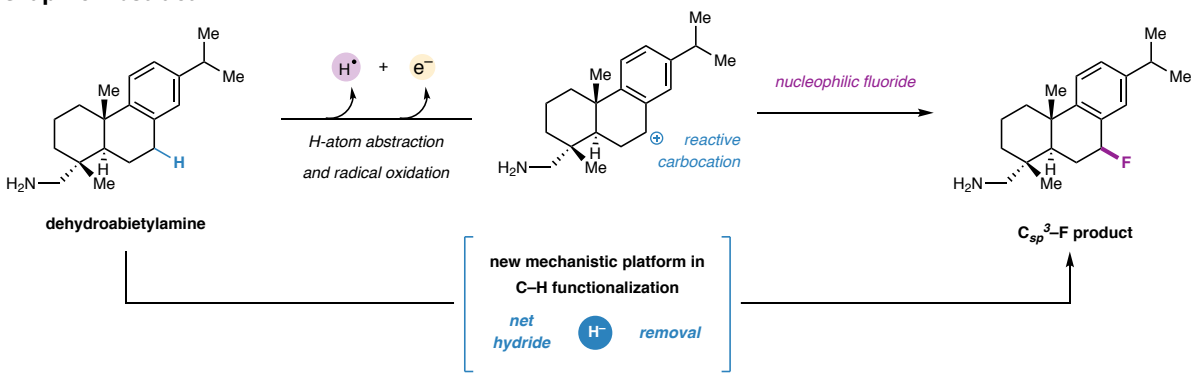
Graphic Abstract: